ARTICLE

# Membrane bending energy and tension govern mitochondrial division

Lina Carlini[1*], Dora Mahecic[1*], Tatjana Kleele[1], Aurélien Roux[2,3], and Suliana Manley[1]

[1] Institute of Physics, École Polytechnique Fédérale de Lausanne (EPFL), Route Cantonale, 1015 Lausanne, Switzerland

[2] Department of Biochemistry, University of Geneva, Geneva, Switzerland

[3] Swiss National Centre for Competence in Research Programme Chemical Biology, Geneva, Switzerland

[*] These authors contributed equally to this work

Correspondence should be addressed to

S.M. (email: suliana.manley@epfl.ch)
Institute of Physics
École Polytechnique Fédérale de Lausanne
Lausanne, Switzerland

1

Mitochondria rely on cellular machinery for their division, which is an essential component of metabolic response of the cell. Many division factors have been identified; however, a framework accounting for the energetic requirements of the mitochondrial fission process is lacking. We report that the presence of an active constriction does not ensure fission. Instead, by measuring constrictions down to ~100 nm with time-lapse super-resolution microscopy, we found that 34% of constrictions failed to divide and 'reversed' to an unconstricted state. Higher local curvatures - reflecting an increased bending energy – made constriction sites more likely to divide, but often with a significant residual energy barrier to fission. Our data suggest that membrane tension, largely arising from pulling forces, could account for this missing energy. These results lead us to propose that mitochondrial fission is probabilistic, and can be modeled as arising from bending energy complemented by a fluctuating membrane tension.

---

Mitochondria are highly dynamic organelles, transported through the cytoplasm along cytoskeletal networks as they change in size and shape. Mitochondrial morphologies can range from a filamentous, connected network to a fragmented collection of individuals. Underlying such morphological changes are altered equilibria between fusion and division[1,2]. These transformations have been linked to an adaptive response to cellular energy requirements, for example in response to stress[3-5] or the cell cycle[6]. As a vestige of their bacterial origins, mitochondria cannot be generated *de novo*, but must multiply by division, or fission, of existing mitochondria[7]. Division has also been suggested to act as part of a quality control mechanism[8,9] and an intracellular signal for mitophagy[10,11].

In bacterial division systems, internal assembly of the fission machinery is tightly regulated and a series of cell cycle checkpoints ensure daughter cell viability. In contrast, the mitochondrial division machinery is external to the organelle, allowing cells to flexibly regulate fission. Initially, the division site is marked by a pre-constriction defined by contact with ER tubules[12] and deformed by targeted actin polymerization[13-15]. Subsequently, dynamin related protein (Drp1)[16,17] is recruited to the site and retained by binding to surface receptors including Mff[18,19] and Fis1[20,21] which accumulate at the division site. Drp1 can oligomerize into helices that wrap around mitochondria, and hydrolyze GTP to provide a mechano-chemical force for constriction[20-22]. The dynamin family protein Dyn2 was also reported to play a role in the final membrane scission[23].

All of these factors combine to deform mitochondria at the constriction site. Intriguingly, pre-constrictions induced by a wide variety of mechanical forces can recruit the mitochondrial fission machinery to result in division[24]. However, it is not known how mitochondria integrate forces imposed by the cytoplasmic machinery to decide whether to divide, or what the physical constraints are underlying mitochondrial fission. This is in part because the relevant physical parameters have not yet been quantified in living cells, hindered by the challenges involved in imaging such dynamic, sub-diffraction limited structures.

Live-cell Structured Illumination Microscopy (SIM) of Drp1-mediated mitochondrial constriction events enabled us to measure dynamic changes in membrane geometry leading up to and following division. We discovered that a fraction of mitochondria constrict dramatically before relaxing to an unconstricted state, termed 'reversals'. Using a custom-written image analysis package and classical elasticity theory, we calculated the energy differences between fission and reversal events, which allowed us to estimate the energy barrier to fission. To investigate the role

of pulling forces from cytoskeletal motors, we used the measured post-divisional recoil of daughter mitochondria to estimate membrane tension based on a viscoelastic model. When we lowered membrane tension by treating cells with nocodazole, we observed increased reversal rates, decreased fission rates and a delay in fission time, underscoring the importance of tension in mitochondrial division. Taken together, our results suggest that mitochondrial fission is a probabilistic process, with elastic energy and tension governing the kinetics and probability of fission.

## Results

### Not all Drp1-mediated constrictions result in fission

We performed live-cell SIM imaging of COS-7 cells transiently transfected with mitochondrial matrix-localized GFP (mito-GFP) and Drp1-mCherry with 1 second temporal resolution. After reconstruction of SIM movies (see Supplementary Information), we observed that Drp1-mCherry marked highly-constricted sites, but while some proceeded to fission, others eventually lost their enrichment of Drp1 and relaxed back to an unconstricted state ('reversal') (Supplementary Movie 1). For the purposes of quantification, we defined 'reversals' (Fig. 1b, d) as instances when a mitochondrion accumulated Drp1 at its constriction site and reached a diameter below 200 nm before relaxing. Overall, 66% of constriction sites with Drp1 proceeded to fission (N=112, Fig. 1a, Supplemental Fig. 1), while the remaining 34% relaxed to an unconstricted state (N=57, Fig. 1b, Supplemental Fig. 2). Similar "reversible" or "non-productive" constrictions were previously observed in yeast[25] and higher eukaryotes[15]. However, the frequency of reversals was not quantified, and the features that distinguished them from fissions were not investigated.

4

To examine whether constriction diameters distinguish fissions and reversals, we followed the temporal evolution of Drp1-mediated constriction sites. On average, fissions and reversals achieved minimum diameters of 120±4 (mean ± standard error, N=61) and 119±5 nm (N=38) respectively (Fig. 1c, e), approaching the resolution limit of SIM. We computed the 95% confidence interval for the difference between mean fission and reversal constriction diameters, and found that these were indistinguishable. Constriction rates in the frames before the smallest diameters were also comparable, increasing to ~ 17 and 18 nm/s respectively, before undergoing fission or reversing (Fig. 1e).

We also imaged mitochondria using live-cell stochastic optical reconstruction microscopy (STORM) with ~ 6-second temporal resolution. Fission and reversal events had negligible differences in their minimum measured diameters, 90±18 (N=13) and 82±10 nm (N=10) respectively (Supplementary Fig. 5a, b), consistent with our SIM data. This agrees well with the sizes of mitochondrial constrictions found with photoactivated localization microscopy (PALM)[26] of mitochondria, and fission and fusion intermediates reported by live-cell STORM[27]. The negligible difference in size between fissions and reversals implies that achieving such diameters is not sufficient for fission. Furthermore, we did not notice significant differences between fission and reversal dynamics, suggesting that the same machinery could be responsible for both.

**Unsuccessful constrictions are not due to a lack of Drp1 or Dyn2**

In seeking to understand what distinguished fissions and reversals, we next examined the fission machinery at Drp1 constriction sites. By quantifying the integrated intensity of Drp1, we found that its accumulation at the constriction site typically coincided with an increased constriction rate (Fig. 1d, f). Furthermore, the constrictions we observed corresponded to the largest diameter at

which Dnm1/Drp1 is proposed to assemble[21,28], supporting a complete molecular assembly on the mitochondrion in the most constricted state. Some sites underwent multiple rounds of constriction coupled with Drp1 accumulation (Fig. 1d), reminiscent of *in vivo* observations of cyclic assembly and disassembly of dynamin at clathrin coated pits[29], and *in vitro* experiments showing cycles of dynamin-[30]mediated constrictions on membrane nanotubes. However, both fissions and reversals displayed cyclic dynamics, 3±2 cycles/min and 2±1 constriction cycles/min respectively (N=61 and 38).

Although Drp1 dynamics did not differentiate fissions and reversals, we wondered whether Dyn2 could[23]. To determine whether reversals are due to a lack of Dyn2, we performed three-color live-cell confocal imaging of mitochondria, Drp1 and Dyn2. We still observed both fissions and reversals, including mitochondrial pre-constrictions which recruited Drp1 and Dyn2, constricted and then relaxed (Supplementary Fig. 5d). To determine whether these events still fulfilled the definition of reversals, we performed live-cell SIM of mitochondria and Dyn2. Constriction sites which reversed in the presence of Dyn2 reached diameters down to ~ 130 nm, close to the resolution limit, confirming that reversal events are not due to a lack of Dyn2. We also noted that while 98% of mitochondria divided at sites marked by the presence of Drp1, only 30 % of those were also enriched in Dyn2 (N=30) (Supplementary Fig. 5e). Overall, no significant differences in constriction diameter, Drp1 or Dyn2 dynamics were observed between fissions and reversals, suggesting that these events are distinct outcomes of a shared, but nondeterministic process.

**Fission events are characterized by a higher bending energy**

The forces exerted by the cytosolic machinery result in deformation of the mitochondrial membrane. Could reversals be a consequence of insufficient deformation at the division site?

6

Although constriction diameters were indistinguishable between fissions and reversals, membrane bending energy is a function of both principal membrane curvatures. These are taken to be the tube and envelope curvatures, under the reasonable approximation that mitochondria are locally axisymmetric (Fig. 2c). Thus, we measured the envelope curvature at mitochondrial constriction sites. Interestingly, fission events maintained a higher magnitude envelope curvature of $(-8.1 \pm 0.5) \cdot 10^{-3}$ nm$^{-1}$ compared to $(-6.4 \pm 0.6) \cdot 10^{-3}$ nm$^{-1}$ in the case of reversals (Fig. 2a,b, N=61 and 38 respectively). To investigate the energetic consequences of this difference, we calculated the bending energy at mitochondrial constriction sites.

From an energetic standpoint, the fission process can be described as a reaction with an energy barrier[32]. We estimated the bending energy, $E_B$, according to the Helfrich equation[31]:

$$E_B = \frac{\kappa}{2} \int J^2 dA \qquad\qquad (1)$$

Here, $\kappa$ is the membrane bending rigidity, $A$ is the membrane area and $J$ is the sum of principal curvatures. The parameter $\kappa$ depends on lipid composition, and is estimated to be 40 $k_B T$ based on *in vitro* measurements of lipid bilayers[32].

We used the measured principal curvatures to estimate the local bending energy around the constriction site (Fig. 2c, Supplementary Fig. 6). Although the energy showed a similar time evolution for both fissions and reversals, the distribution of fission energies was shifted to higher values (Fig 2d,e, insert values ±SEM, N=53 and 31 respectively). Nevertheless, there was significant overlap between the distributions, indicating that a range of bending energies can result in either outcome (Fig. 2f). We speculate that bending energy contributes to overcoming the energy barrier to fission, making constrictions with higher bending energy more likely to divide. This idea is supported by the experimentally measured probability of fission, defined as the ratio of the

number of fissions to total constrictions with a given energy, which increases with local bending energy (Fig. 2f). Importantly, the energy distribution of fission events coupled with the experimental probability allowed us to estimate the energy barrier at ~250 kT, corresponding to energy above which we observe no reversal activity (Fig. 2f). Considering mitochondria are double-membraned organelles, this value is consistent with previous reports for dynamin mediated scission[33], as well as theoretical estimates of the energy barrier for a hemifusion state, from which fission follows spontaneously[34].

**Pharmacological decrease of membrane tension decreases probability of fission**

We noticed that after division, daughter mitochondria would recoil from each other, in a directed manner away from the division site. This motion was distinct from their normal mobility, and was consistent with what one would expect when cutting an elastic body under tension. We hypothesized that the daughter mitochondrial might be pulled apart by an external force. Hence another contribution in the form of membrane tension would further increase the elastic energy at the constriction site. To estimate this tension, we measured the initial speed of recoil of post-divisional mitochondria, and used a visco-elastic model[15] (Fig. 3a) to infer the pulling force $\boldsymbol{F}$. While it has been proposed to play a role in separating mitochondria after fission is achieved[35], the contribution of pulling forces to fission has not been explored. This is in part because these forces have never been measured. As previously implemented for dividing cells[36], the relationship between force and recoil velocity, $\boldsymbol{v}$ is:

$$\boldsymbol{F} = \frac{\eta v}{l_0}\boldsymbol{\pi r^2} \qquad (2)$$

where $\eta$ is the mitochondrial viscosity, $r$ is the constriction radius and $l_0$ is the deformation length. The membrane tension, $\boldsymbol{\tau,}$ is then calculated by dividing the measured force by the

circumference of the constriction site, $\tau = \frac{F}{2\pi r}$, and provides an estimate of the membrane tension immediately prior to fission.

As mitochondrial transport is mainly mediated through microtubule based motor proteins[37,38], we hypothesized that the external pulling force could be exerted by the same motors. To test the role of microtubule motor-induced membrane tension in inducing fission, we depolymerized microtubules using nocodazole[39,40]. Indeed, estimated tensions were reduced by 40%, reflecting a decrease in recoil velocities and pulling forces (Fig. 3b, N=33 DMSO control and 26 nocodazole).

Importantly, the rate of Drp1-induced constrictions per mitochondrial area remained the same ($\sim$ 0.014 $\text{min}^{-1}\mu\text{m}^{-2}$), suggesting that Drp1 recruitment and constriction activity were not perturbed by nocodazole treatment. However, we found a 2.4-fold increase in the rate of reversal events (Fig. 3e), and a concomitant decrease in the rate of fission. This is in agreement with previous reports that nocodazole decreases fission rates[41]. Examining more closely the measured probability of fission, we found it was shifted towards higher bending energies for nocodazole-treated cells (Fig 3f), implying that to achieve similar probability of fission would now require more deformation from Drp1 or other cellular machinery. Consistent with this, fission in nocodazole-treated cells occurred at constriction sites with on average higher bending energies, ~40 kT higher than untreated cells (Fig. 3d, N=33 control and 22 nocodazole). We also noticed that Drp1 appeared to reside for longer periods of time at the constriction sites of mitochondria in nocodazole-treated cells. To estimate the time needed for division, we defined the start time to be the onset of rapid constriction, which was consistently coupled with a Drp1 signal increase or stabilization, and the end time by division itself (Supplemental Fig. 7). Fission events in nocodazole-treated cells required on average ~12±7 s longer (Fig. 3c, N=33 control and 22 nocodazole).

**Mitochondrial fission as a probabilistic process**

Our measurements show that fission occurs over a wide range of bending energies, tensions, and time scales. Components of the cellular machinery, including Drp1, coordinate to deform the membrane, and while many sites undergo fission within the first 20 seconds of rapid constriction, others take 4-5 times as long. However, the fission machinery does not maintain a constriction indefinitely and can disassemble within this timeframe, resulting in constrictions that do reverse, especially sites with lower bending energies and tensions. Models developed for other fission processes, such as dynamin-mediated endocytosis, explain the distribution of fission times as an outcome of a stochastic, thermally activated process[33] which allows the membrane energies to fluctuate over the energy barrier to fission. Membranes with higher elastic energy, and thus lower residual energies, will undergo fission more rapidly. In the case of mitochondria, we estimated that the residual energy barrier from bending energy to fission fell in the range of tens of $k_BT$ on average (Supplemental Information). This is too large a barrier to be overcome by thermal fluctuations alone, so how do these constrictions succeed in fission?

By pharmacologically decreasing membrane tension, we observed slower fission times and a shifted experimental probability of fission (Fig. 3b,f), demonstrating that tension is important in driving the final step of fission. However, tension takes on a wide range of values, (Fig. 3b), and we expect that it fluctuates in time as mitochondria diffuse, migrate, and interact with different cellular structures. Based on this, we suggest that fluctuations in tension, rather than thermal energy, provide most of the stochastic energy to overcome the energy barrier (SI). If this is the case, tension should help set the time of fission. This model predicts that the average time, $\langle t_f \rangle$ to undergo fission is set by the residual energy, $\Delta E$, between the constricted and hemi-fission states:

$$\langle t_f \rangle \propto \exp\left(\frac{\Delta E}{kT}\right) \tag{3}$$

In agreement with a stochastic tension-activated model, average fission times show an exponential dependence on bending energy[33] (Fig. 4a).

We propose a probabilistic model of mitochondrial fission, where bending energy (achieved by Drp1 and Dyn2) and tension (generated primarily by microtubule-based motor proteins) determine fission probability (Fig 4b). Bending energy at the constriction site sets the distance to the energy barrier. Separately, tension sets the range of stochastic fluctuation energies available to overcome the energy barrier. As predicted, with a nocodazole-induced decrease in tensions, fewer fluctuations are large enough overcome the fission barrier, which increases fission times and lowers the probability of fission. Within this model, any constriction will have a probability of undergoing fission, depending on its distance from the energy barrier and the available fluctuation energies (Fig 4b).

## Discussion

The mitochondrial division machinery is composed of multiple force-generating elements, including the cytoskeleton, other organelles, and Drp1/Dyn2 assemblies. These elements interact in a complex manner and their activity may depend on context, giving rise to cell-specific differences. In this work, we set out to develop a unifying physical framework to explain how mitochondria integrate these forces to decide whether, and when to divide. To account for our observations of the dynamic changes in mitochondria during constriction and scission, we have developed a model in which the membrane tension and bending energy of a constriction predict its probability and timing of fission. Such a model can be readily adapted to include contributions from other, as yet unknown molecular or cell-type and context specific factors. The non-

deterministic nature of mitochondrial division is supported by the existence of "reversal" events, in which Drp1 actively constricts before releasing mitochondria without scission occurring.

We considered the contributions of two components to the probability of fission: (1) bending energy and (2) membrane tension.

(1) The fate of a mitochondrial constriction depends on the local membrane curvature, a feature that is also important for positioning dynamin-mediated endocytosis[33]. Successful fission events are characterized by a higher deformation at the constriction site, which implies increased energy used to bend the membrane. By calculating the energy differences between fission and reversal events, we estimated the energy barrier that needs to be overcome for fission to occur. The molecular mechanisms for deforming mitochondrial membranes include the known cytosolic machinery: the ER, actin, Drp1, and Dyn2. However, mitochondria might also possess internal mechanisms that generate curvature such as accumulation of negatively curved lipids, like cardiolipin[42], at the constriction site to promote fission. Indeed, a dominant negative Drp1-mutation, which does not interact with cardiolipin, leads to lower fission rates[43]. Furthermore, the bending rigidity of the plasma membrane has recently been estimated at a higher value of ~ 35 kT per lipid bilayer[44], which would further underline the importance of bending energy.

(2) Microtubule motor proteins provide a mechanical force and can increase membrane tension, impacting fission in endocytosis[45,46]. Similarly, we found that a pharmacological destabilization of the microtubule cytoskeleton results in a lower mitochondrial membrane tension and leads to increased reversal rates, decreased fission rates and slower fission times. This not only identifies the microtubule cytoskeleton as an additional factor providing mechanical force for division, but also underscores the contribution of membrane tension for overcoming the energy barrier to fission.

Mitochondrial fission contrasts with many other fission processes since it requires the scission of two membranes. Our model considers the two membranes together, as a composite elastic sheet with a mean geometry, and is sufficient to capture the timing and probabilities of fission. Nevertheless, we expect fission of the inner membrane will occur first, since its bending energy is geometrically constrained to be higher. Sequential timing is required for a non-leaky fission process, which is predicted[35,43], to avoid inadvertently triggering apoptosis or disruption of membrane potential[47]. Fission of the outer membrane could then follow due to a sudden increase in the local stress after breaking of the inner membrane. In the future, it will be important to develop tools to discern inner and outer membranes to better understand how information is transduced through the mitochondrial envelope.

The probabilistic nature of mitochondrial fission is interesting, since most other division processes are deterministic, where assembly of the division machinery irreversibly leads to division. It raises the question, what is the underlying biological function of a probabilistic division? At first glance, it appears inefficient that the cell assembles the molecular machinery, and provides the energy to strongly constrict mitochondria, yet they sometimes fail to divide. But perhaps this could allow cells to adjust mitochondrial fission rates rapidly, by altering the probability for fission without changing expression levels. We speculate that regulating fission by modulating the bending energy or the longevity of constriction sites by post-translational modifications to Drp1[48-50] or altering pulling forces and membrane tension induced by $Ca^{2+}$-dependent mitochondrial transport[51-53] could achieve this. Future experiments are needed to investigate whether and how extracellular stimuli can alter mitochondrial network morphology by changing the probability of fission.

## METHODS

For Methods, please see Supplementary Information online.

## ACKNOWLEDGEMENTS

## AUTHOR CONTRIBUTIONS

L.C., D.M., T.K, A.R. and S.M. designed the experiments. L.C., D.M., T.K. and S.M. performed the experiments. L.C., D.M. and T.K. analyzed the data. L.C. and D.M. wrote the software code. L.C., D.M., T.K., A.R. and S.M. wrote the manuscript.

## COMPETING INTEREST

The authors declare no competing financial interests.

**FIGURE LEGENDS**

**Figure 1: Drp1 mediated constrictions show similar constriction diameter and Drp1 intensity kinetics regardless of whether they undergo fission or reverse.**

(a,b) Time-lapse SIM imaging of COS-7 cells transiently transfected with mito-GFP (grey) and mCh-Drp1 (magenta) showing (a) fission and (b) reversal events (see Supplementary Movies 1,2, Supplemental Figures 1,2). (c) Dynamic evolution of diameter at the mitochondrial constriction site measured for fission (blue) and reversal (red) events shown above. (d) Normalized integrated intensity of Drp1 at the constriction site over time measured for fission (blue) and reversal (red) events shown above. (e) Binned curves showing the evolution of the constriction diameter for fissions (blue, n= 61) and reversals (red, n= 38). Inset shows the distribution of minimal diameters of fission and reversals at t=0 (horizontal line shows mean) (f) Binned curves showing normalized integrated intensity of Drp1 at the constriction site in fissions (blue, n=61) and reversals for fissions and reversals (red, n=38). Error bars present s.d. (light shade) and s.e.m. (dark shade). Scale bar represents 500 nm in a and b. Statistical significance calculated by 2-tailed Mann-Whitney U test: n.s. indicates p≥0.05.

**Figure 2: High envelope curvature at the constriction site increases the local bending energy and probability of fission**

(a) Binned curves showing the evolution of envelope curvature at the constriction site for fissions (blue, n= 61) and reversals (red, n= 38). Shaded regions represent s.d. (light shade) and s.e.m. (dark shade). (b) Distribution of envelope curvatures at t=0 for fissions and reversals (horizontal line represents mean). (c) Analysis of the principal curvatures of the constriction site allowed estimation of the local bending energy, at the length scale maximizing the energy density. (d)

15

Binned curves for the calculated local bending energies over time for fissions (blue, n= 61) and reversals (red, n= 38). (e) Distribution of bending energies at t= 0 for fissions and reversals. (f) Left: Histogram showing numbers of fissions and reversals at different local bending energy intervals. Right: Experimental probability of fission calculated from ratio of fissions to total constrictions at different local bending energy intervals. Statistical significance calculated by 2-tailed Mann Whitney U test: *P<0.05, ***P<0.001.

**Figure 3: Membrane tension contributes to the probability and timing of fission.**

(a) Time-lapse SIM images of a mitochondrion (labelled with mito-GFP) 1 sec before (left) and after (right) fission showing the recoil of daughter mitochondria post fission which was used to infer membrane tension at the constriction site. Red line marks the constriction site. Measured retraction speeds were projected onto the white dashed line, perpendicular to the constriction site (red line). (b) Pre-treatment with 10µM Nocodazole significantly lowered the tension measured from retractions in comparison with control DMSO treated samples. (c,d) Nocodazole treatment resulted in (c) shifted fission times and (d) bending energy distributions compared to controls (horizontal line shows mean). (e)Box chart showing rates of fission and reversal rates in Nocodazole treated (N=16) and control (N=16) cells. (f) Experimental probability of fission for Nocodazole treated and control cells. Scale bar: 1µm. Statistical significance calculated by 1- and 2-tailed Mann-Whitney U test where appropriate: *P<0.05; **P<0.01.

**Figure 4: Probabilistic model of mitochondrial fission is controlled by bending energy and membrane tension.**

(a) Fission time as a function of bending energy. The bending energy was averaged over the last 3 frames before fission. Squares represent the average values within different local bending energy intervals. Grey dots represent a subset of the original data points. Error bars represent the s.e.m. Fit curve y=a*exp(-x/b) with a=23 s and b=45 kT. (b) Cartoon of the probabilistic model of mitochondrial fission showing the contribution of bending energy and membrane tension in reaching the energy barrier for fission. Bending energy is the main contribution to overcoming the energy barrier and increases steadily during mitochondrial constriction to bringing the membrane elastic energy close to the energy barrier to fission (green trajectory). After constriction, energy fluctuations due to tension can overcome it (shaded region). Both bending energy and tension set the probability p of a constriction undergoing fission (blue trajectory). Reversals occur either due to a lack of bending energy or low probability of necessary fluctuation energies such as low tensions induced by nocodazole (dotted red trajectory).

## REFERENCES

1    Nunnari, J. *et al.* Mitochondrial transmission during mating in Saccharomyces cerevisiae is determined by mitochondrial fusion and fission and the intramitochondrial segregation of mitochondrial DNA. *Mol Biol Cell* **8**, 1233-1242 (1997).

2    Bleazard, W. *et al.* The dynamin-related GTPase Dnm1 regulates mitochondrial fission in yeast. *Nat Cell Biol* **1**, 298-304 (1999).

3    Tondera, D. *et al.* SLP-2 is required for stress-induced mitochondrial hyperfusion. *EMBO J* **28**, 1589-1600 (2009).

4    Gomes, L. C., Benedetto, G. D. & Scorrano, L. During autophagy mitochondria elongate, are spared from degradation and sustain cell viability. *Nat Cell Biol* **13**, 589-598, (2011).

5    Rambold, A. S., Kostelecky, B., Elia, N. & Lippincott-Schwartz, J. Tubular network formation protects mitochondria from autophagosomal degradation during nutrient starvation. *Proc. Natl. Acad. Sci. USA* **108**, 10190-10195, (2011).

6    Mitra, K., Wunder, C., Roysam, B., Lin, G. & Lippincott-Schwartz, J. A hyperfused mitochondrial state achieved at G1-S regulates cyclin E buildup and entry into S phase. *Proc Natl Acad Sci U S A* **106**, 11960-11965 (2009).

7    Youle, R. J. & van der Bliek, A. M. Mitochondrial fission, fusion, and stress. *Science* **337**, 1062-1065 (2012).

8    Garrido, N. *et al.* Composition and Dynamics of Human Mitochondrial Nucleoids. *Mol Biol Cell* **14**, 1583-1596 (2003).

9    Ban-Ishihara, R., Ishihara, T., Sasaki, N., Mihara, K. & Ishihara, N. Dynamics of nucleoid structure regulated by mitochondrial fission contributes to cristae reformation and release of cytochrome c. *Proc Natl Acad Sci U S A* **110**, 11863-11868, (2013).

10 Twig, G. *et al.* Fission and selective fusion govern mitochondrial segregation and elimination by autophagy. *EMBO J* **27**, 433-446 (2008).

11 Burman, Jonathon L. *et al.* Mitochondrial fission facilitates the selective mitophagy of protein aggregates. *J Cell Biol* **216**, 3231-3247 (2017).

12 Friedman, J. R. *et al.* ER Tubules Mark Sites of Mitochondrial Division. *Science* **334**, 358-362 (2011).

13 Korobova, F., Ramabhadran, V. & Higgs, H. N. An Actin-Dependent Step in Mitochondrial Fission Mediated by the ER-Associated Formin INF2. *Science* **339**, 464-467 (2013).

14 Manor, U. *et al.* A mitochondria-anchored isoform of the actin-nucleating spire protein regulates mitochondrial division. *Elife* **4**, e08828 (2015).

15 Ji, W. K., Hatch, A. L., Merrill, R. A., Strack, S. & Higgs, H. N. Actin filaments target the oligomeric maturation of the dynamin GTPase Drp1 to mitochondrial fission sites. *Elife* **4**, e11553 (2015).

16 Labrousse, A. M. *et al.* C. elegans Dynamin-Related Protein DRP-1 Controls Severing of the Mitochondrial Outer Membrane. *Mol Cell* **4**, 815-826, (1999).

17 Smirnova, E., Griparic, L., Shurland, D.-L. & Bliek, A. M. v. d. Dynamin-related Protein Drp1 Is Required for Mitochondrial Division in Mammalian Cells. *Mol Biol Cell* **12**, 2245-2256 (2001).

18 Gandre-Babbe, S. & van der Bliek, A. M. The novel tail-anchored membrane protein Mff controls mitochondrial and peroxisomal fission in mammalian cells. *Mol Biol Cell* **19**, 2402-2412 (2008).

19 Otera, H. *et al.* Mff is an essential factor for mitochondrial recruitment of Drp1 during mitochondrial fission in mammalian cells. *J Cell Biol* **191**, 1141-1158 (2010).

20 Ingerman, E. *et al.* Dnm1 forms spirals that are structurally tailored to fit mitochondria. *J of Cell Biol* **26**, 1021-1027 (2005).

21 Mears, J. A. *et al.* Conformational changes in Dnm1 support a contractile mechanism for mitochondrial fission. *Nat Struct Mol Biol* **18**, 20-26 (2011).

22 Fröhlich, C. *et al.* Structural insights into oligomerization and mitochondrial remodelling of dynamin 1-like protein. *EMBO J,* 1280-1292 (2013).

23 Lee, J. E., Westrate, L. M., Wu, H., Page, C. & Voeltz, G. K. Multiple dynamin family members collaborate to drive mitochondrial division. *Nature* **540**, 139-143 (2016).

24 Helle, S. C. J. *et al.* Mechanical force induces mitochondrial fission. *Elife* **6**, e30292 (2017).

25 Legesse-Miller, A. Constriction and Dnm1p Recruitment Are Distinct Processes in Mitochondrial Fission. *Mol Biol Cell* **14**, 1953-1963 (2003).

26 Rosenbloom, A. B. *et al.* Optimized two-color super resolution imaging of Drp1 during mitochondrial fission with a slow-switching Dronpa variant. *Proc Natl Acad Sci U S A* **111**, 13093-13098 (2014).

27 Shim, S. H. *et al.* Super-resolution fluorescence imaging of organelles in live cells with photoswitchable membrane probes. *Proc Natl Acad Sci U S A* **109**, 13978-13983 (2012).

28 Basu, K. *et al.* Molecular mechanism of DRP1 assembly studied in vitro by cryo-electron microscopy. *PloS one* **12**, 1-21 (2017).

29 Galli, V. *et al.* Uncoupling of dynamin polymerization and GTPase activity revealed by the conformation-specific nanobody dynab. *eLife* **6** (2017).

30 Bashkirov, P. V. *et al.* GTPase cycle of dynamin is coupled to membrane squeeze and release, leading to spontaneous fission. *Cell* **135**, 1276-1286 (2008).

31 Helfrich, W. Elastic properties of lipid bilayers: theory and possible experiments. *Z Naturforsch C* **28**, 693-703 (1973).

32 Niggemann, G., Kummrow, M. & Helfrich, W. The Bending Rigidity of Phosphatidylcholine Bilayers: Dependences on Experimental Method, Sample Cell Sealing and Temperature. *J Phys France* **5**, 413-425 (1995).

33 Morlot, S. *et al.* Membrane Shape at the Edge of the Dynamin Helix Sets Location and Duration of the Fission Reaction. *Cell* **151**, 619-629 (2012).

34 Kozlovsky, Y. & Kozlov, M. M. Membrane Fission: Model for Intermediate Structures. *Biophys J* **85**, 85-96 (2003).

35 Ugarte-Uribe, B., Müller, H. M., Otsuki, M., Nickel, W. & García-Sáez, A. J. Dynamin-related protein 1 (Drp1) promotes structural intermediates of membrane division. *J Biol Chem* **289**, 30645-30656 (2014).

36 Lafaurie-Janvore, J. *et al.* ESCRT-III Assembly and Cytokinetic Abscission Are Induced by Tension Release in the Intercellular Bridge. *Science* **339**, 1625-1629 (2013).

37 Hirokawa, N. Kinesin and Dynein Superfamily Proteins and the Mechanism of Organelle Transport. *Science* **279**, 519-526 (1998).

38 Nangaku, M. *et al.* KIF1B, a novel microtubule plus end-directed monomeric motor protein for transport of mitochondria. *Cell* **79**, 1209-1220 (1994).

39 Hoebeke, J., Van Nijen, G. & De Brabander, M. Interaction of nocodazole (R 17934), a new anti-tumoral drug, with rat brain tubulin. *Biochem Biophys Res Commun* **69**, 319-324 (1976).

40 De Brabander, M. J., Van de Veire, R. M., Aerts, F. E., Borgers, M. & Janssen, P. A. The effects of methyl (5-(2-thienylcarbonyl)-1H-benzimidazol-2-yl) carbamate, (R 17934; NSC

238159), a new synthetic antitumoral drug interfering with microtubules, on mammalian cells cultured in vitro. *Cancer research* **36**, 905-916 (1976).

41  Woods, L. C., Berbusse, G. W. & Naylor, K. Microtubules Are Essential for Mitochondrial Dynamics–Fission, Fusion, and Motility–in Dictyostelium discoideum. *Front Cell Dev Biol* **4** (2016).

42  Stepanyants, N. *et al.* Cardiolipin's propensity for phase transition and its reorganization by dynamin-related protein 1 form a basis for mitochondrial membrane fission. *Mol Biol Cell* **26**, 3104-3116 (2015).

43  Montessuit, S. *et al.* Membrane remodeling induced by the dynamin-related protein Drp1 stimulates Bax oligomerization. *Cell* **142**, 889-901 (2010).

44  Lieber, A. D., Schweitzer, Y., Kozlov, M. M. & Keren, K. Front-to-rear membrane tension gradient in rapidly moving cells. *Biophys J* **108**, 1599-1603 (2015).

45  Day, C. A. *et al.* Microtubule Motors Power Plasma Membrane Tubulation in Clathrin-Independent Endocytosis. *Traffic* **16**, 572-590 (2015).

46  Renard, H.-F. *et al.* Endophilin-A2 functions in membrane scission in clathrin-independent endocytosis. *Nature* **517**, 493-496 (2014).

47  Hatch, A. L., Gurel, P. S. & Higgs, H. N. Novel roles for actin in mitochondrial fission. *J Cell Sci* **127**, 4549-4560 (2014).

48  Braschi, E., Zunino, R. & McBride, H. M. MAPL is a new mitochondrial SUMO E3 ligase that regulates mitochondrial fission. *EMBO Rep* **10**, 748-754 (2009).

49  Cribbs, J. T. & Strack, S. Reversible phosphorylation of Drp1 by cyclic AMP-dependent protein kinase and calcineurin regulates mitochondrial fission and cell death. *EMBO Rep* **8**, 939-944 (2007).
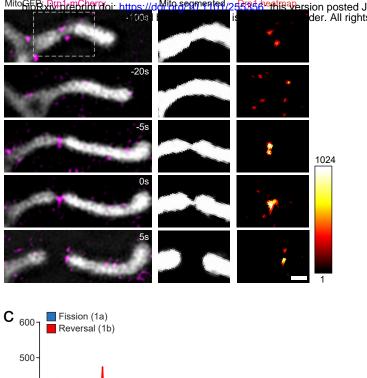
50  Taguchi, N., Ishihara, N., Jofuku, A., Oka, T. & Mihara, K. Mitotic phosphorylation of dynamin-related GTPase Drp1 participates in mitochondrial fission. *J Biol Chem* **282**, 11521-11529 (2007).

51  Yi, M., Weaver, D. & Hajnóczky, G. Control of mitochondrial motility and distribution by the calcium signal: A homeostatic circuit. *J Cell Biol*, 661-672 (2004).

52  MacAskill, A. F. *et al.* Miro1 Is a Calcium Sensor for Glutamate Receptor-Dependent Localization of Mitochondria at Synapses. *Neuron* **61**, 541-555 (2009).

53  Wang, X. & Schwarz, T. L. The Mechanism of Ca2+-Dependent Regulation of Kinesin-Mediated Mitochondrial Motility. *Cell* **136**, 163-174 (2009).
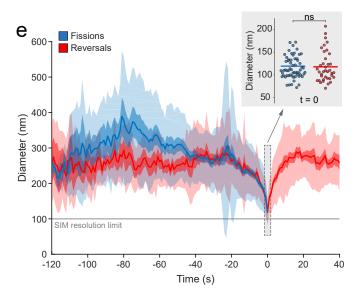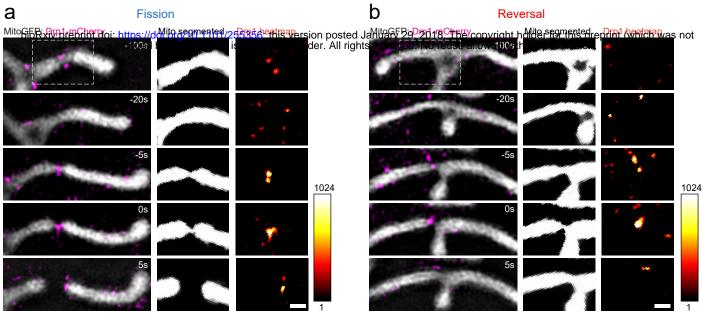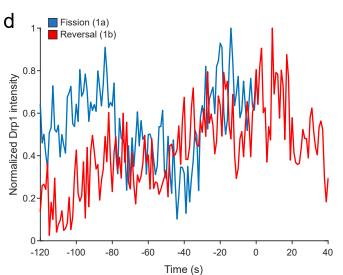
Carlini et al, Figure 1

Carlini et al, Figure 2

Carlini et al, Figure 3

a

b



Carlini et al, Figure 4